A Machine Learning approach for DVCS identification without proton detection

Juan Sebastian Alvarado

IJCLab - Orsay

International workshop on CLAS12 physics and future perspectives at JLab
22/03/2023

Introduction

In principle, the measurement of only an electron and a photon is enough to reconstruct a DVCS event. We aim for DVCS event reconstruction without requiring final proton information.

Advantages (with respect to $ep\gamma$ detection):

- Gives access to a wider phase space for GPD studies.
  - Improves GPD studies at low $-t$.
  - Higher statistics, hence more precise BSA measurements.
- Helpful for experiments that do not consider proton detection such as RG-H with transversely polarized NH_3 target (see Marco's presentation).

Difficulties:

- The $ep\gamma$ final state includes background contributions from the whole Deep Inelastic Scattering (DIS) spectra.
- Reduced options for cuts:
  - Only one exclusivity variable: Missing mass of $ep \to e\gamma$.

Therefore, we need a method that ensures DVCS identification: Machine Learning

We test the ML approach on experimental data:

1. Validation of the method when we include the proton information.
2. Application to the case without proton information.

$ep \to e\gamma p$: Data selection

Analyzed data set

- RG-A data: unpolarized liquid hydrogen target.
- Inbending torus configuration
- No restriction on the detection topology of the particles.

Kinematic window:

- $W > 2$ GeV,
- $Q^2 > 1$ GeV^2 ,
- $\mathbf{q}' > 2$ GeV (photon),
- $\mathbf{k}' > 1$ GeV (electron),
- $\mathbf{p}' > 0.3$ GeV (nucleon).

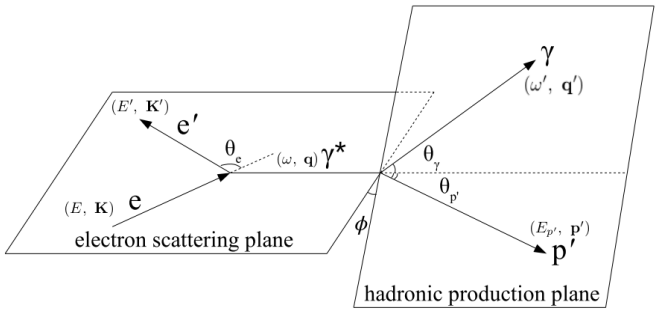

Exclusivity cuts:

We reconstruct ϕ and t in two ways:

1. Using $\gamma*$ and the outgoing photon γ: $\Rightarrow \phi(\gamma)$
2. Using $\gamma*$ and the recoil proton p: $\Rightarrow \phi(p')$

- $\Delta\phi = |\phi(p') - \phi(\gamma)| < 2°$,
- $\Delta t = |t(p') - t(\gamma)| < 2$ GeV^2,
- $\mathbf{P}_{miss} < 1$ GeV.

Event selection:

- No restriction on the number of particles in the event or detection topology.
- If multiple e, γ or p detections, we select the set (e, γ, p) that minimizes the missing mass of the process $ep \to ep\gamma$

$ep \to e\gamma p$: Model training

The main contamination channel is $ep \to ep\pi^0 \to ep\gamma(\gamma)$.

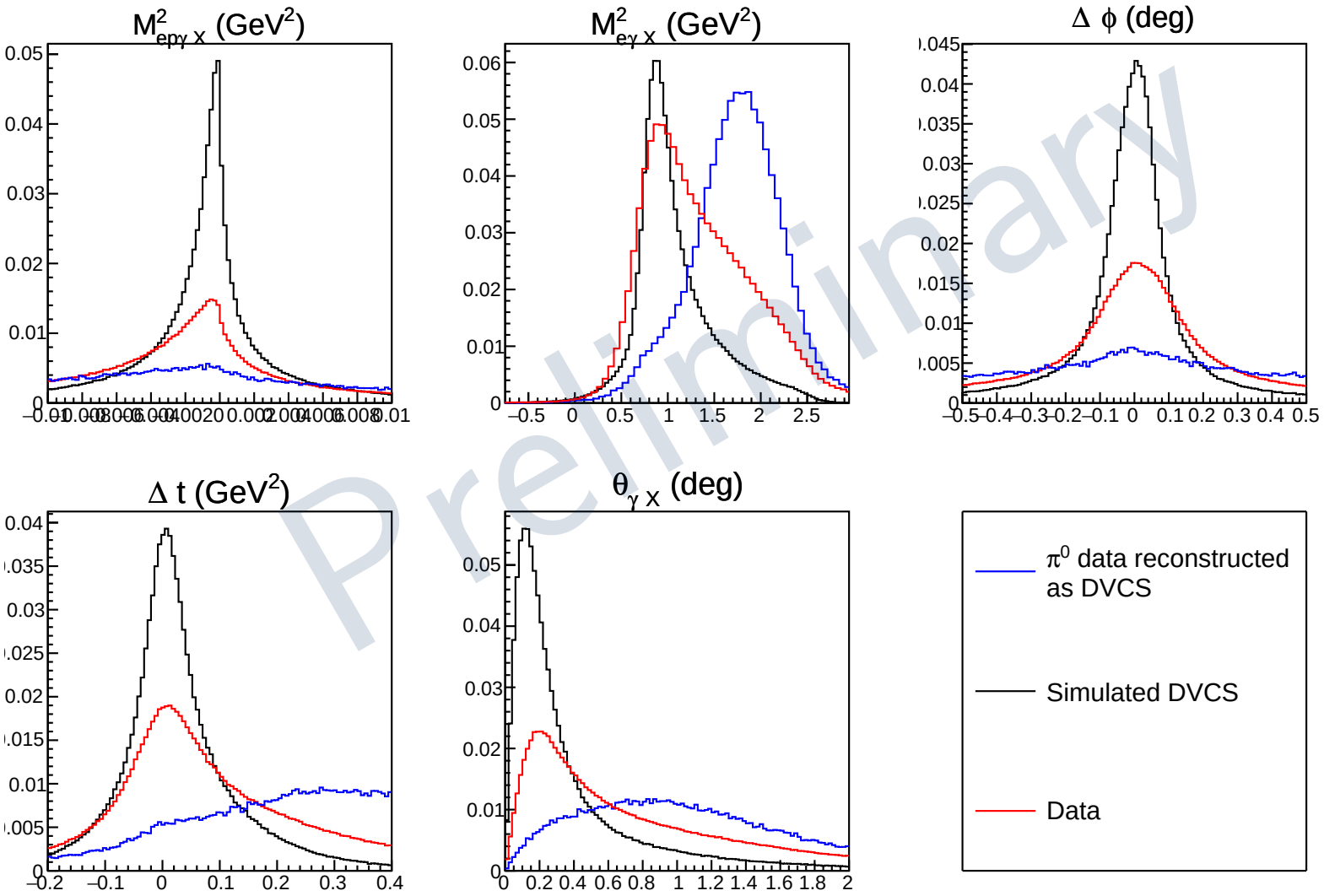

$ep \to e\gamma p$: Background subtraction

To optimize the DVCS event selection, a Boosted Decision Tree (BDT) is trained to classify the events.

- Discriminating variables: $\{M^2_{ep\gamma}, M^2_{e\gamma}, \Delta\phi, \Delta t, \theta_{\gamma X}\}$.
- Simulated DVCS as signal.
- π^0 production data, reconstructed as DVCS, as background.

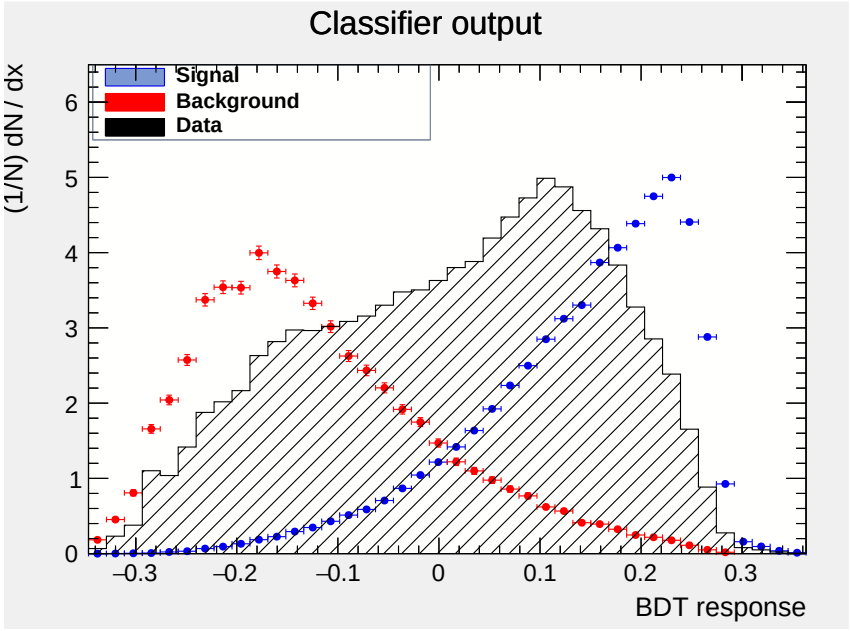

(a) BDT output distributions for different datasets.

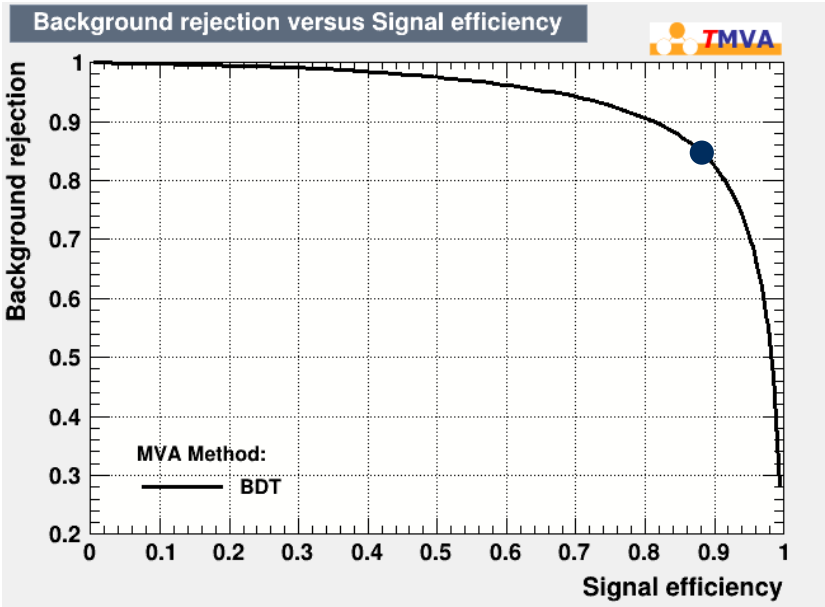

(b) ROC curve of the model and applied cut.

$ep \to e\gamma p$: Background substraction

We extract a dataset with 89.67% DVCS and 10.32% DVMP.

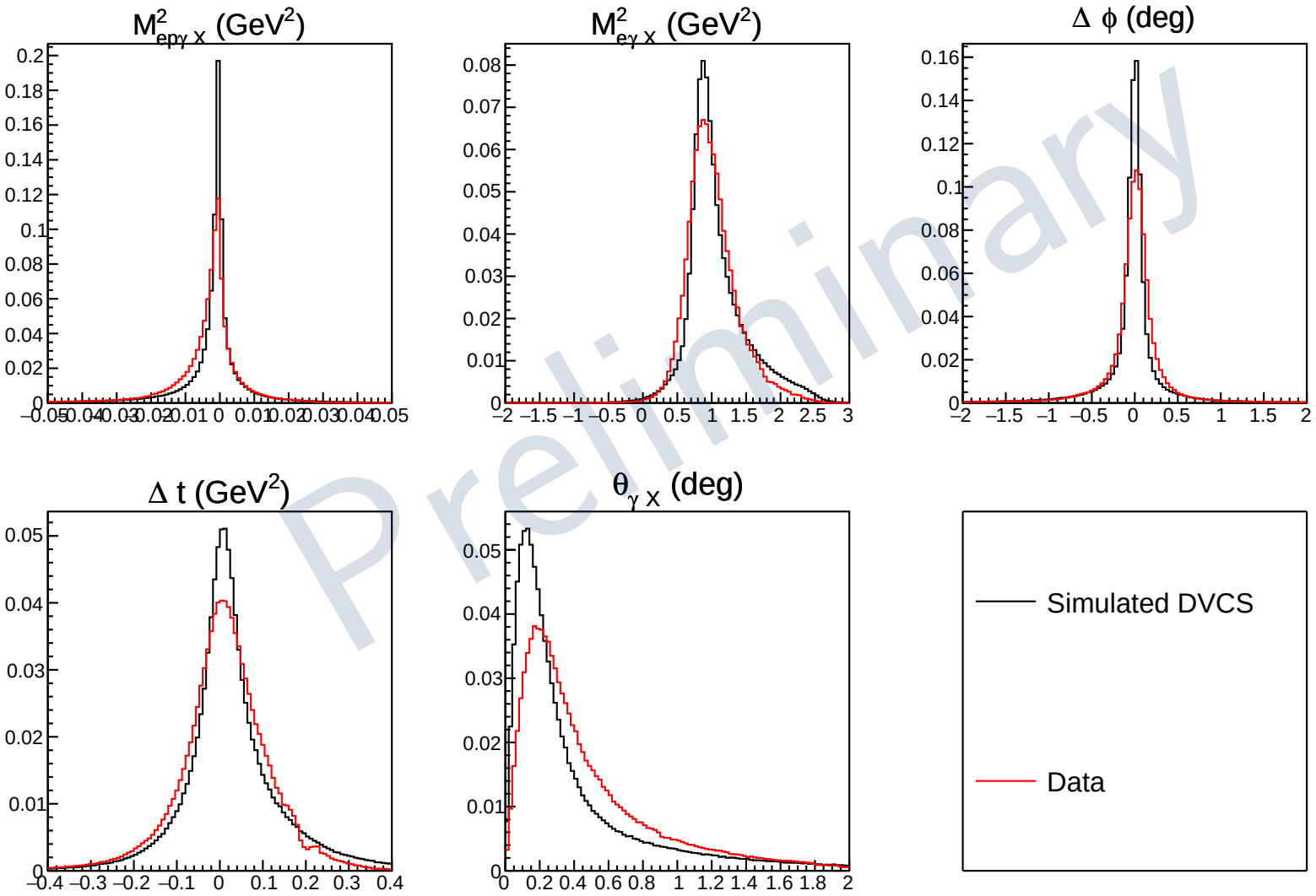

$ep \to e\gamma(p)$: Data selection

Kinematic window:
We apply the same kinematic restrictions:

- $W > 2$ GeV,
- $Q^2 > 1$ GeV^2 ,
- $\mathbf{q}' > 2$ GeV (photon),
- $\mathbf{k}' > 1$ GeV (electron).
- $-\frac{t}{Q^2} < 1$,

Exclusivity cuts:
However, our exclusivity cuts are no longer useful.

- ~~$\Delta\phi = |\phi(p) - \phi(\gamma)| mod(180) < 2°$~~,
- ~~$\Delta t = |t(p) - t(\gamma)| < 2$ GeV^2~~,
- ~~$\mathbf{P}_{miss} < 1$ GeV~~.

Event selection

- Only analyze events with 1 or 2 photons.
- The event is selected by taking the most energetic photon and electron.

BDT training:

- Training for π^0 and general DIS backgrounds.
- Discriminating variables: $\{M^2_{e\gamma X}, M^2_{eX}, M^2_{\gamma X}\}$.
- Dataset is splitted in two:
  - Events where the photon is in the FT ($\theta_\gamma < 5°$)
  - Events where the photon is in the FD ($\theta_\gamma > 5°$)

$ep \to e\gamma(p)$: Model training

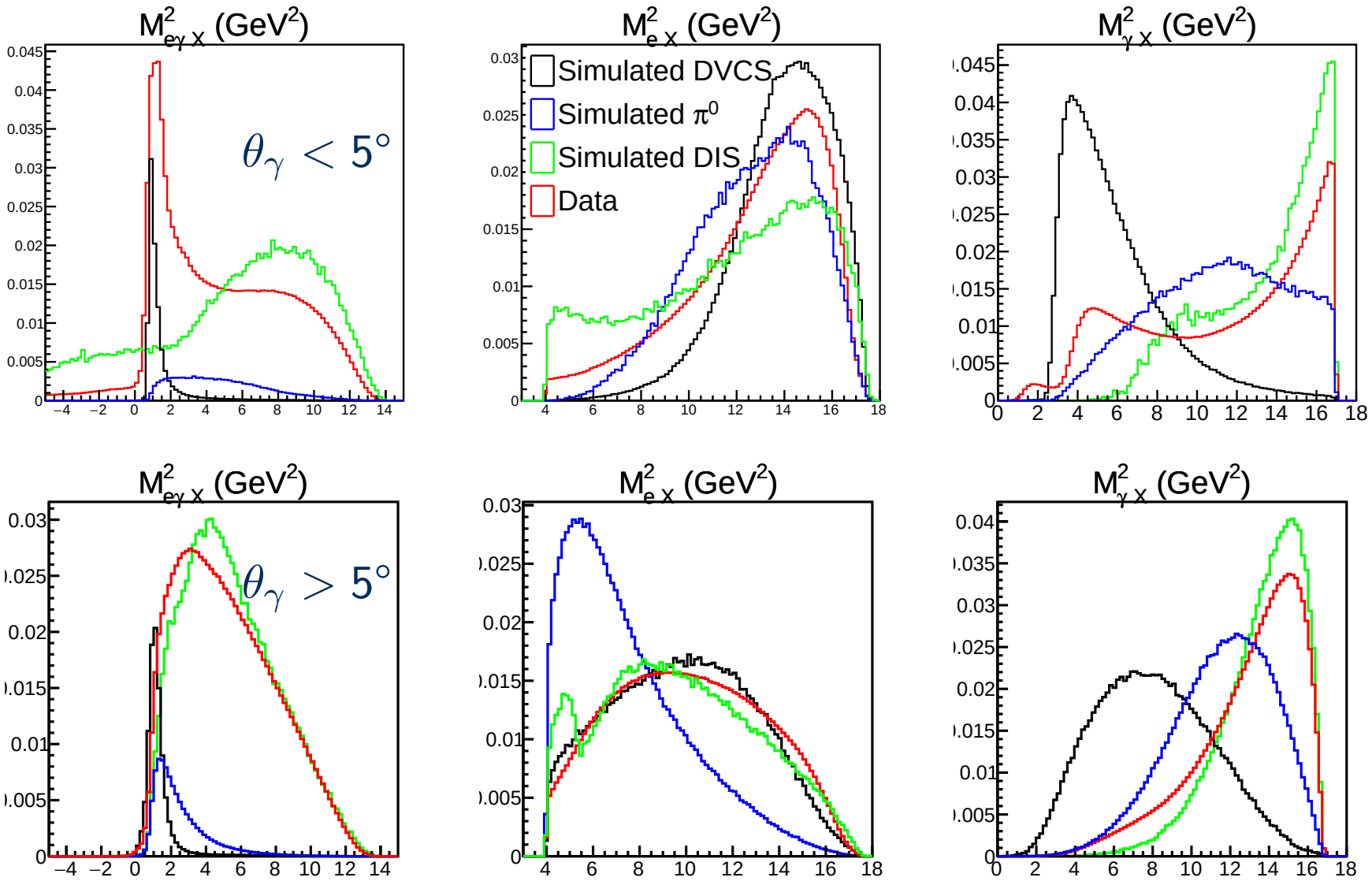

$ep \to e\gamma(p)$: Background subtraction

The training of the BDT results in:

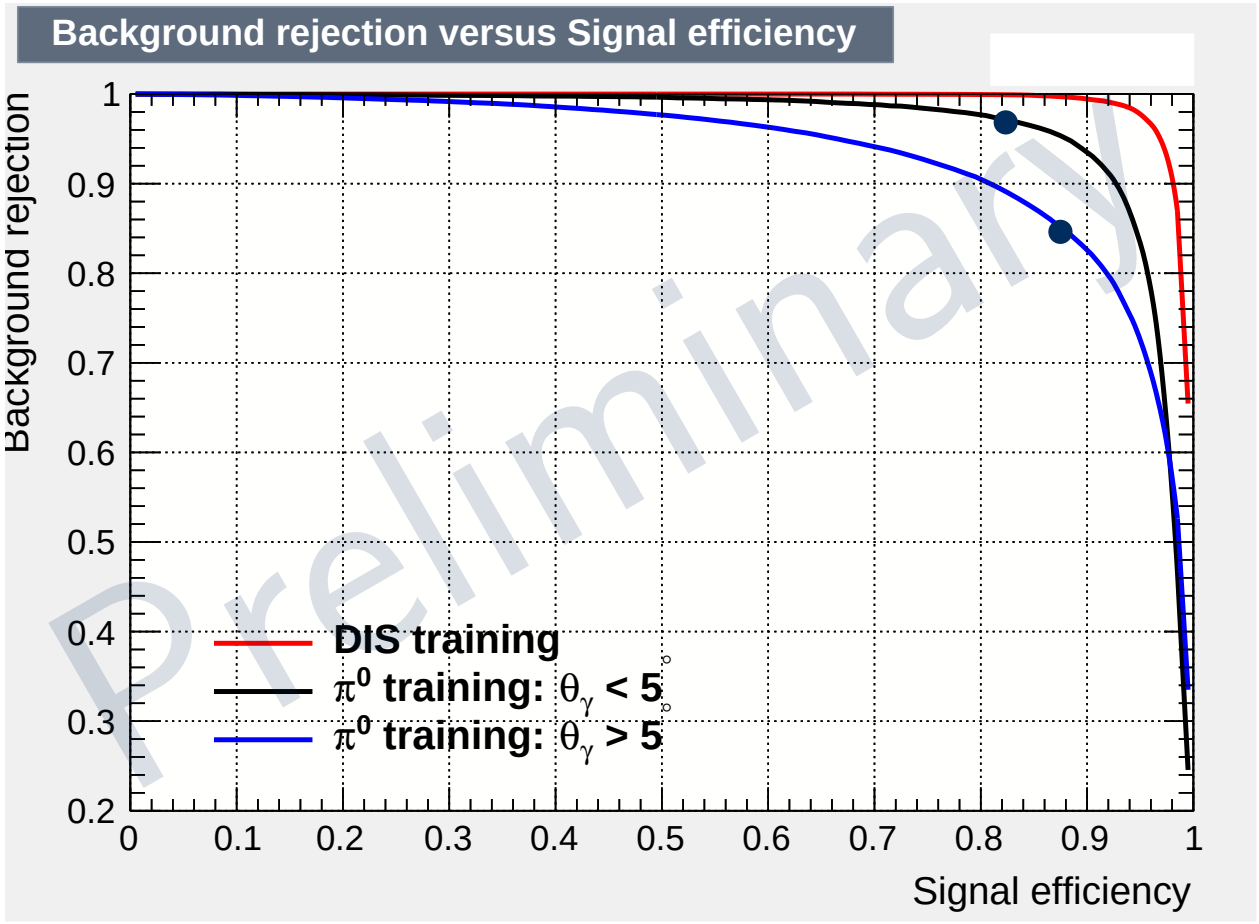

Figure: ROC curve of the model for the DIS and π^0 background trainings indicating the applied cut. DIS training gives similar results in both cases.

$ep \to e\gamma(p)$: Comparison with $e\gamma p$ detection

There are more events in general, mostly in the small t region.

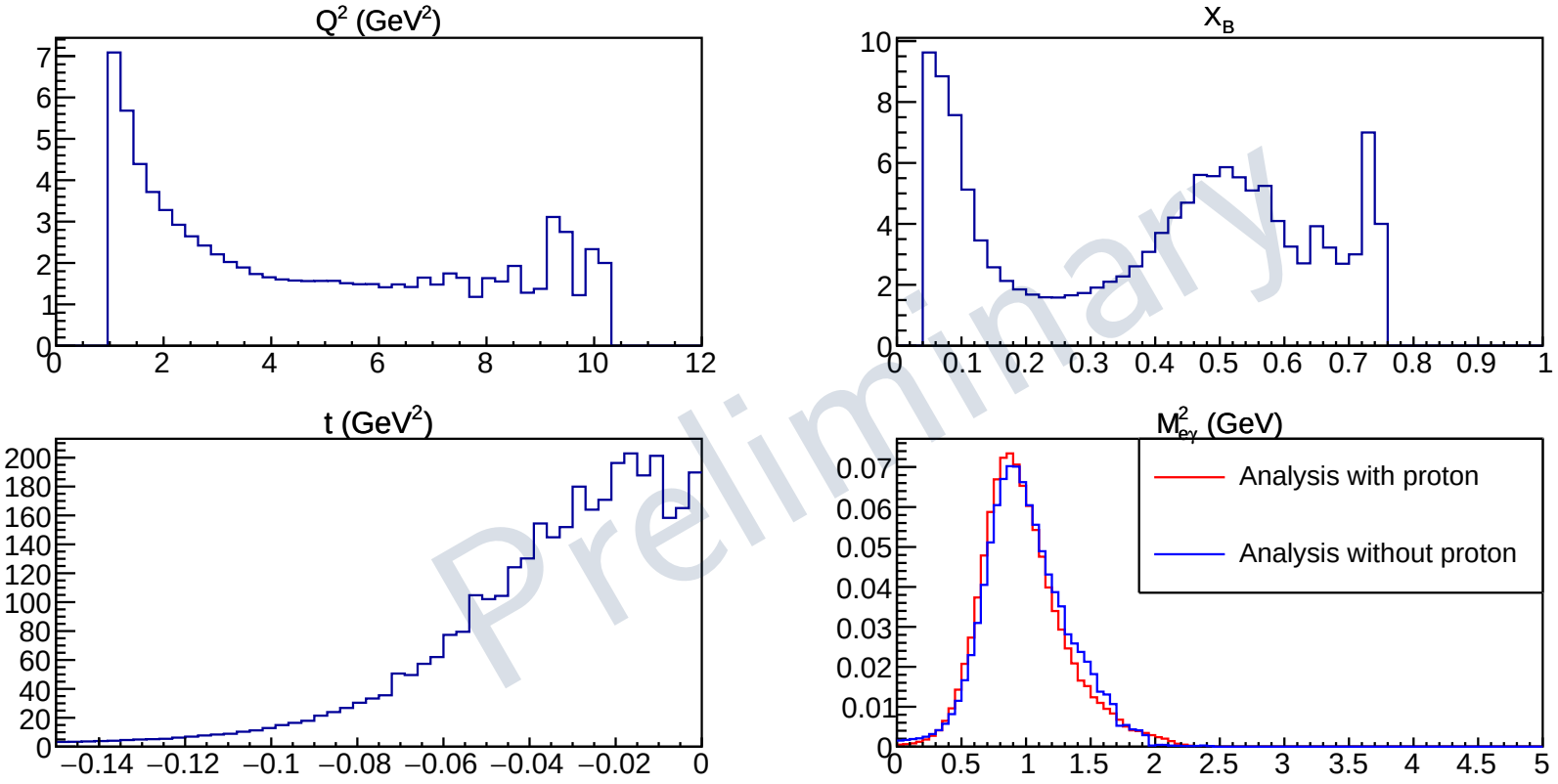

$\frac{\text{No proton}}{\textit{proton}}$ ratios and $M^2_{e\gamma X}$ for $\theta_\gamma < 5°$

$ep \to e\gamma(p)$: Comparison with $e\gamma p$ detection

There are more events in general, mostly in the small t region.

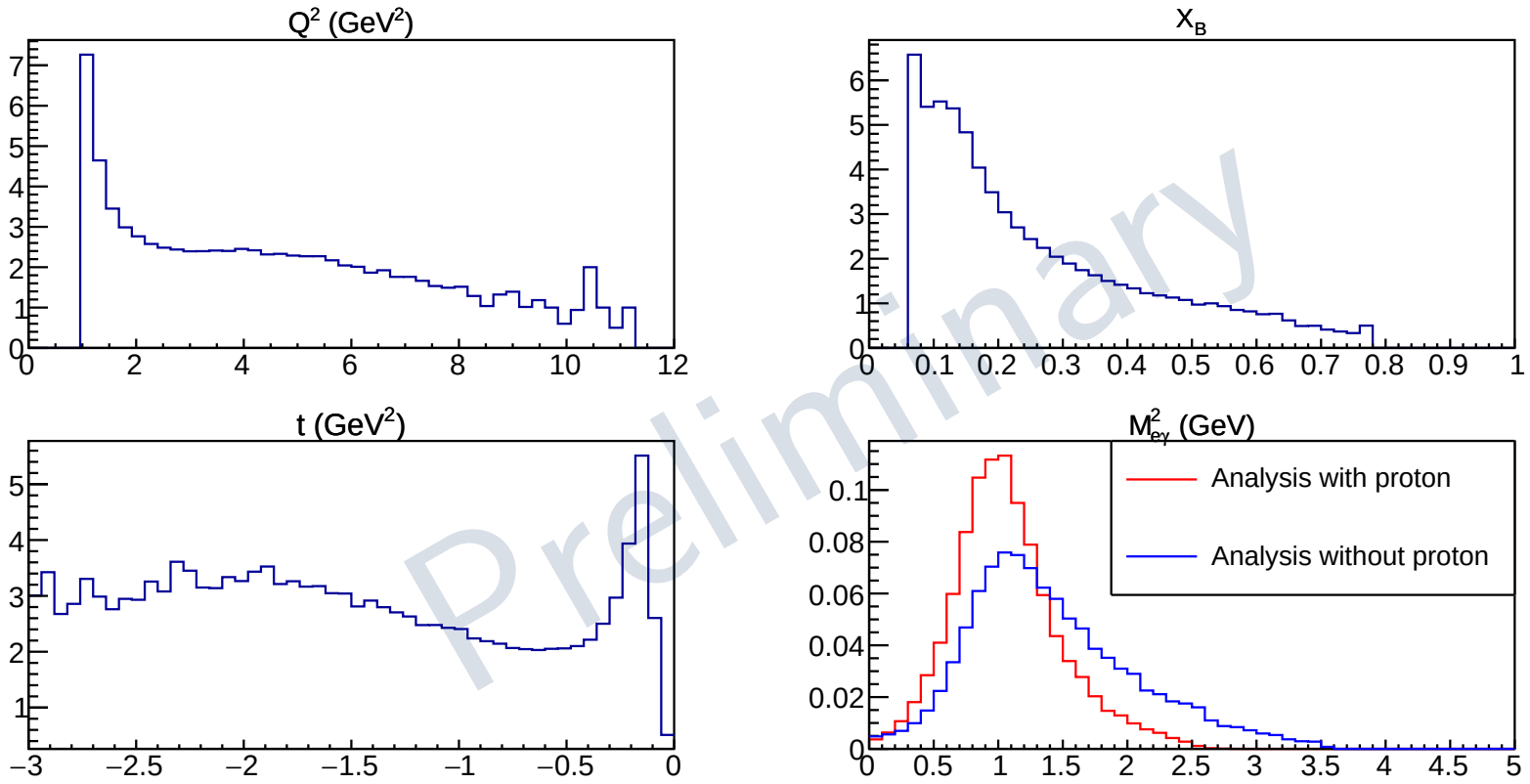

No proton:proton ratios and $M^2_{e\gamma X}$ for $\theta_\gamma > 5°$

Beam Spin Asymmetry

We construct bins of equal number of events before background substraction

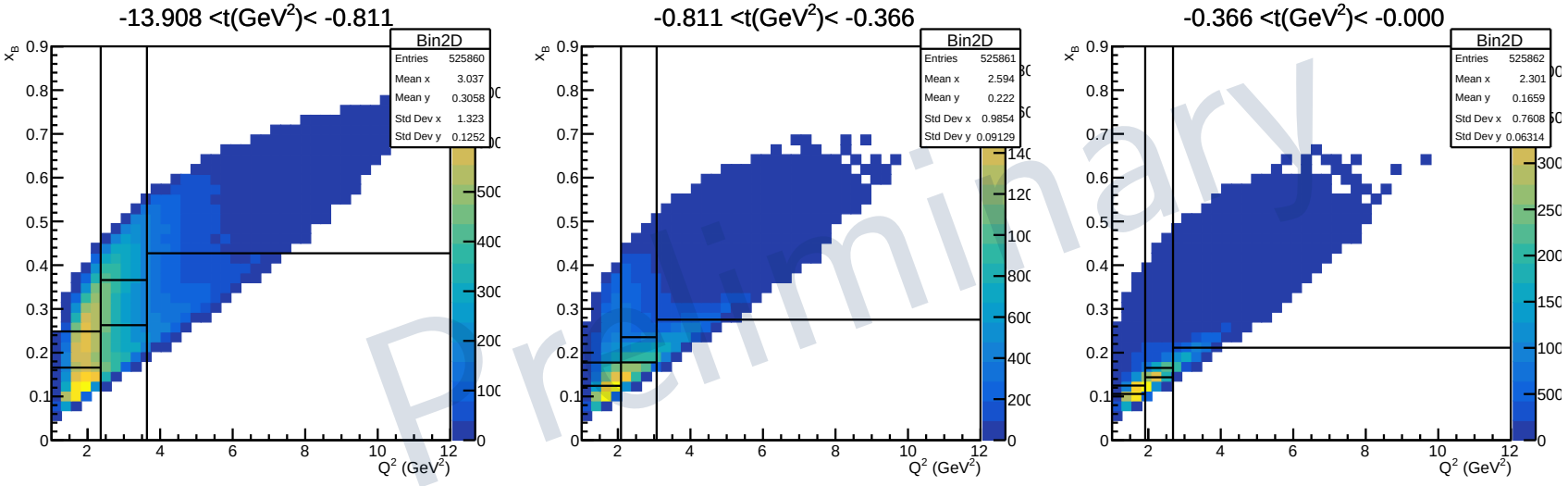

Figure: Binning scheme for BSA measurements in regions with $60K$ events.

Raw Beam Spin Asymmetry

$$A_{LU} \equiv \frac{1}{P}\frac{h^+ - h^-}{h^+ + h^-} \sim \frac{p_0 \ \sin(\phi)}{1 + p_1 \ \cos(\phi)} \sim \frac{\sin(\phi)}{\sigma_{UU}} \Im \left[F_1 \mathcal{H} + \xi(F_1 + F_2)\tilde{\mathcal{H}} - kF_2\mathcal{E} + ... \right]$$

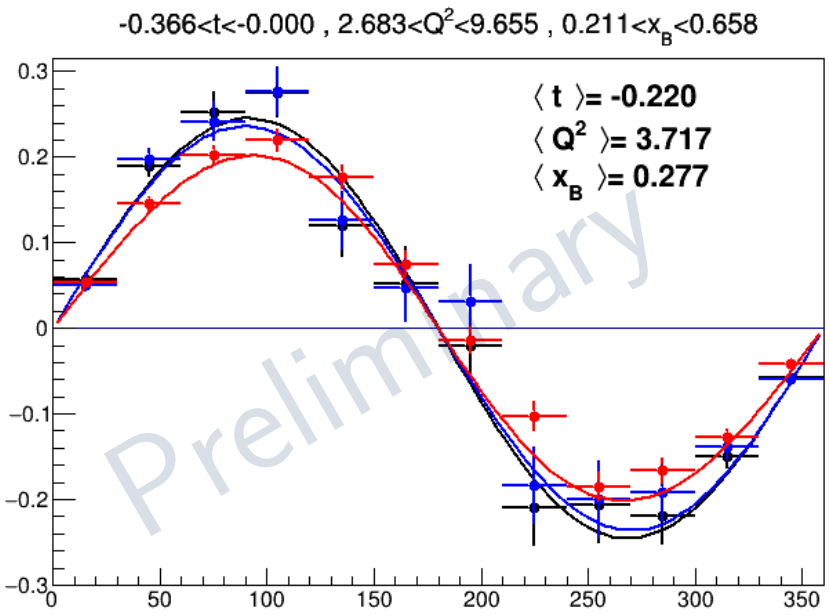

	GP	BP	GNP
$\langle t \rangle$ (GeV)^2	-0.251	-0.247	-0.220
$\langle Q^2 \rangle$ (GeV)^2	3.753	3.759	3.717
$\langle x_B \rangle$	0.260	0.264	0.277

- Global training with proton (blue): GP
- **Binned training with proton (black)**: BP
- Global training without proton (red): GNP

- Training on bins gives very similar results to the global training.
- Training without proton information has an additional systematic shift.

Raw Beam Spin Asymmetry

Now, comparing with a measurement from a previous CLAS12 analysis*.

$1.8\ \text{GeV}^2 < Q^2 < 2.4\ \text{GeV}^2$ $\quad 0.16 < x_B < 0.26$ $\quad t > -0.2\ \text{GeV}^2$

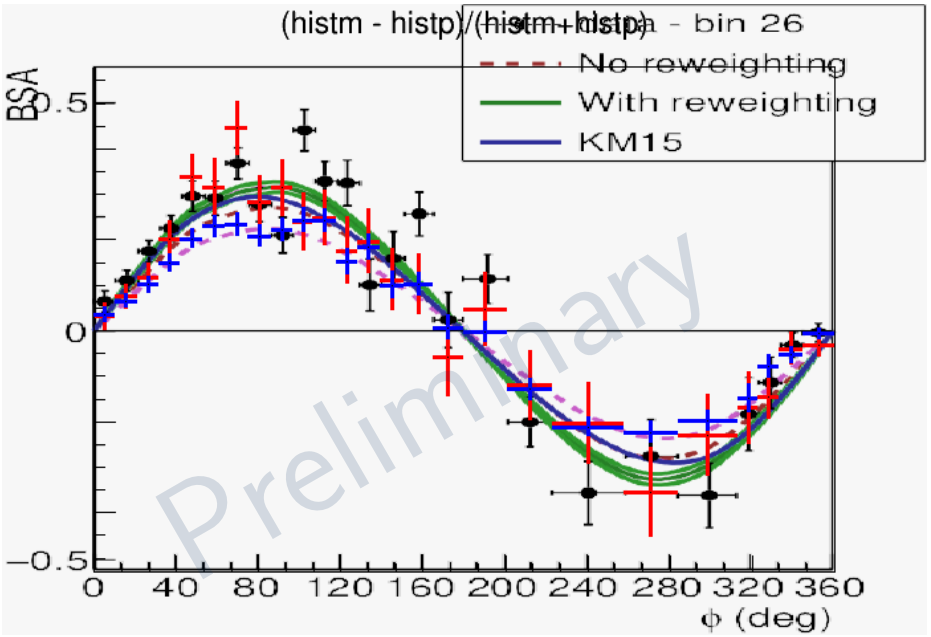

	Proton	No proton
$\langle t \rangle$ (GeV^2)	-0.138	-0.117
$\langle Q^2 \rangle$ (GeV^2)	2.156	2.111
$\langle x_B \rangle$	0.191	0.193

- BSA measurement from CLAS12 **analysis note (black)**.
- Raw** BSA from the current analysis with proton detection (red)
- Raw** BSA from the current analysis without proton detection (blue)

*G. Christiaens et al. "Deeply Virtual Compton Scattering on proton: Beam Spin Asymmetry extraction". In: CLAS12 Analysis Note (2021).
** Before subtraction of the residual π^0 contamination.

Conclusions

- Boosted decision trees presents an alternative for channel selection on an event-by-event basis.
- When the final proton is included:
  - DVCS exclusivity variables have a sufficient separation power to allow DVCS and Deep Exclusive π^0 Production identification in an efficient way.
  - Without any restriction on the detection topology and including proton information, a dataset with $\sim 90\%$ DVCS events can be extracted.
  - Training on kinematical bins is not strictly needed.
- When the final proton information is ignored:
  - There is a strong contribution of DIS processes to the background.
  - We can recover more events, in comparison to the proton-detected case, and directly benefits the small t region.
  - We have smaller statistical error bars on the BSA measurements.
- In general, leftover contamination has to be subtracted.

Outlook

- Subtraction of leftover contamination.
- Implementation of other background subtraction methods.
  - Sweights technique (see Pivk, M., & Le Diberder, F. R. (2005). Nucl. Instrum, 555(1-2), 356-369.).
- RG-H preparations (see Marco's presentation)
  - Transversely polarized NH_3 target experiment.
  - Detector configuration only includes the forward detector.
- Analysis of data from deuterium target.
  - Test the method for neutron DVCS identification.

Thanks

ML approach: Boosted Decision Trees (BDT)

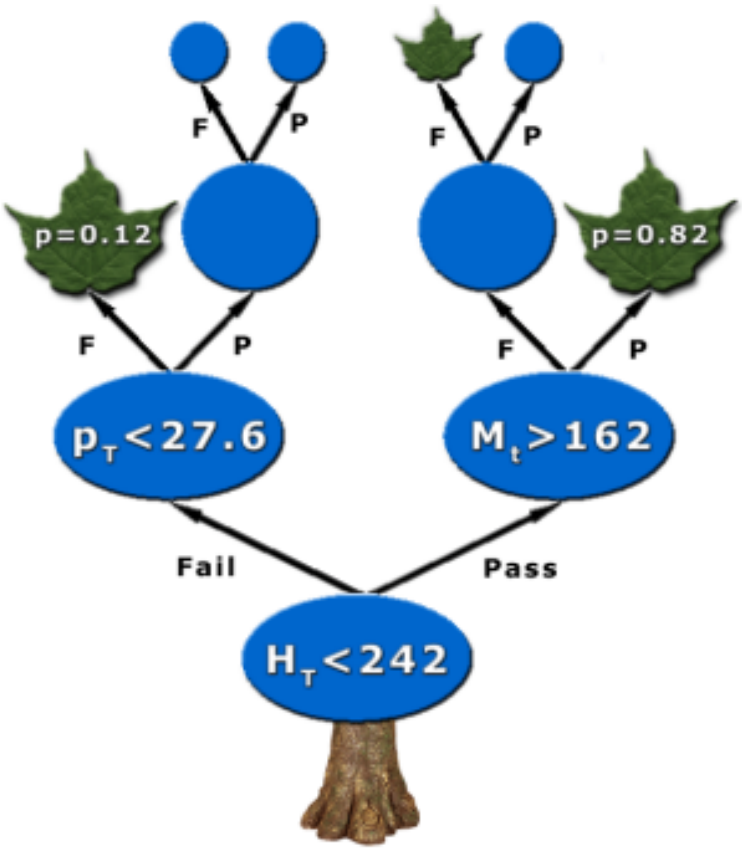

Taken from Coadou, Yann. EPJ Web of conferences. Vol. 55. EDP Sciences, 2013.

A decision tree:

- Scans the given variables looking for the point with maximum separation between classes.
- Splits the data recursively until each event lies on a terminal node (leaf) and assigns it a score.

Additionally, boosting is:

- Train iteratively a decision tree.
- At each step, focus the training on misclassified events.
- Final classification is based on the majority of votes.

$ep \to e\gamma p$: Background subtraction

A look to the kinematics:

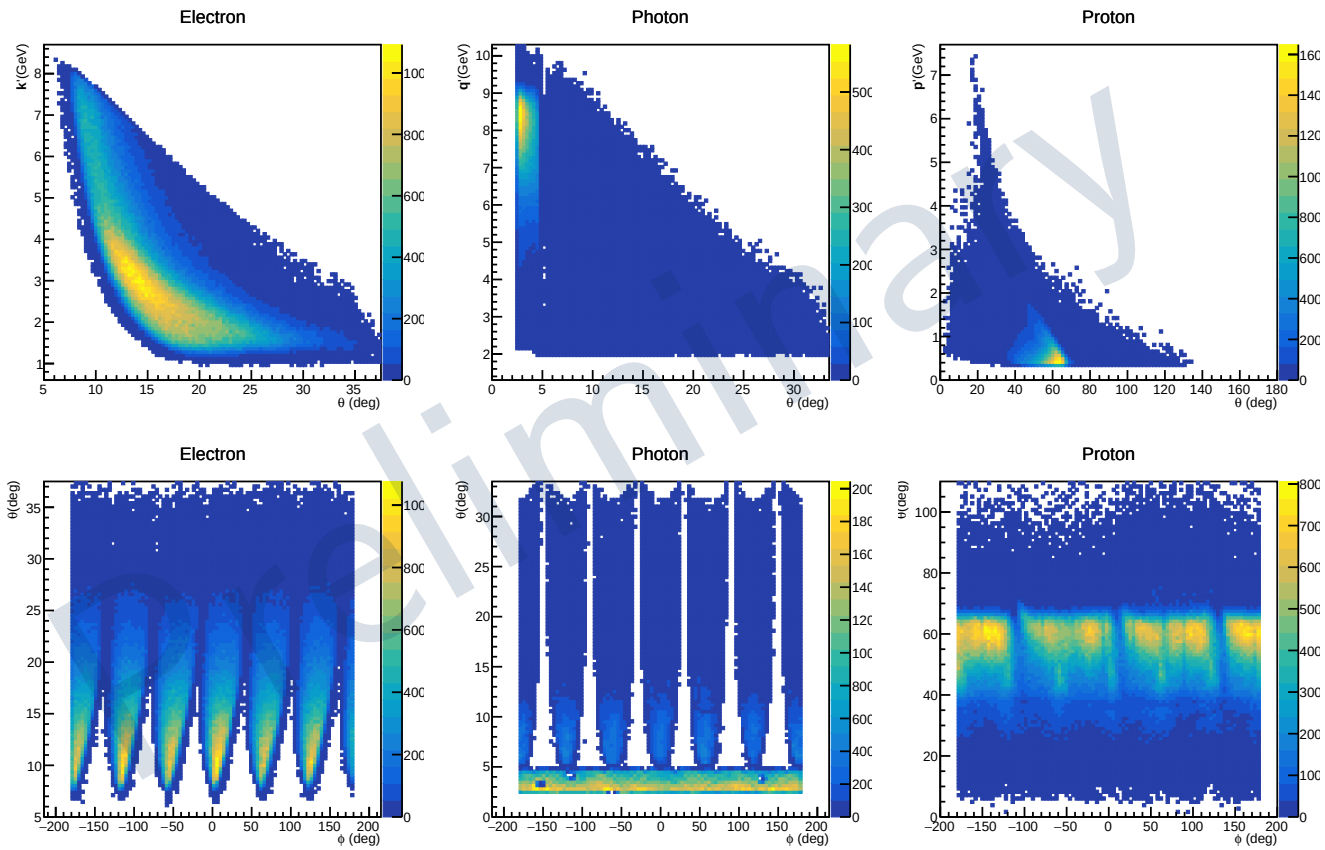

Figure: Momentum of the final particles as a function of the polar angle (first row) and detection polar vs azimuthal angle for each final state particle (second row).

$ep \to e\gamma(p)$: Background subtraction

Let's finally look at the kinematics of the extracted dataset

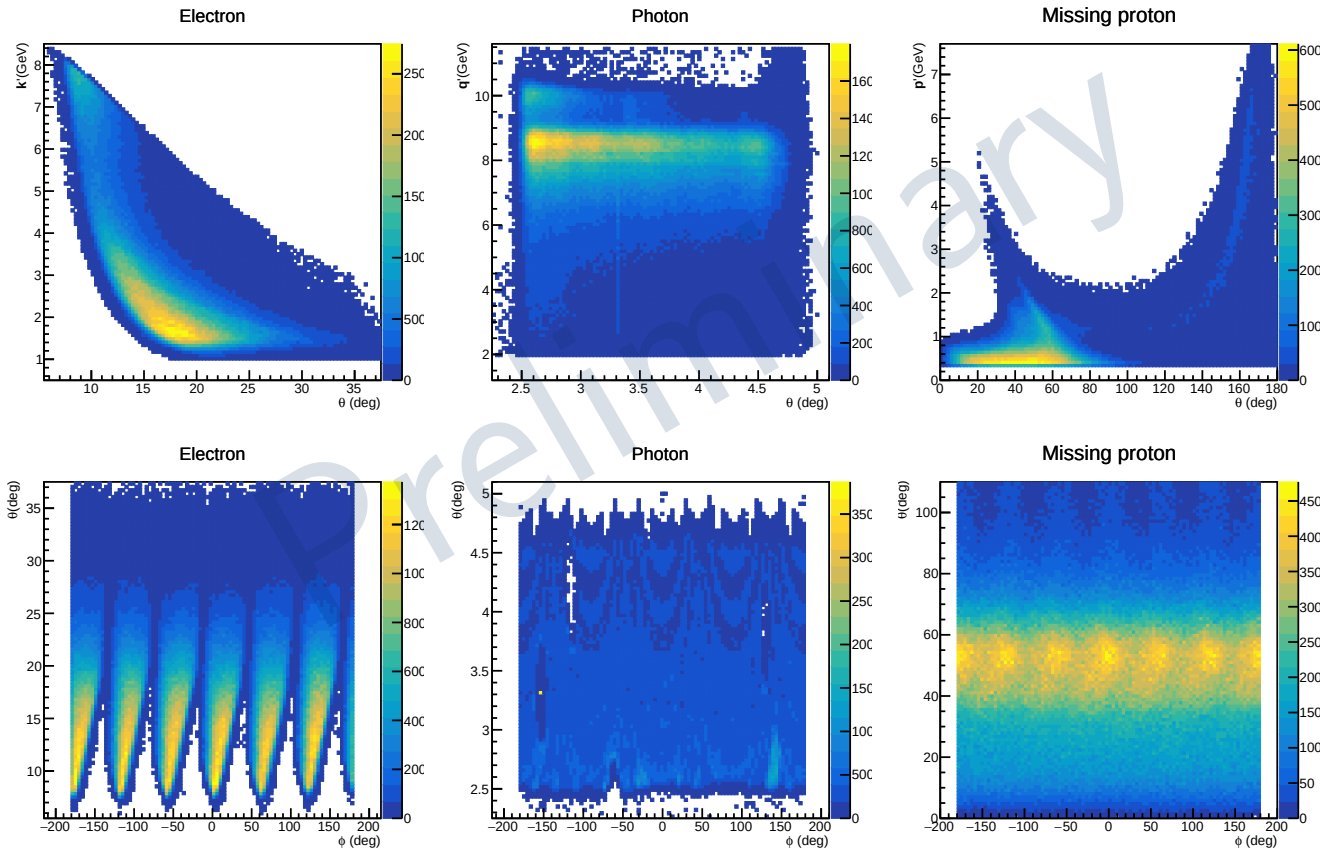

Figure: Momentum of the final particles as a function of the polar angle (first row) and detection polar vs azimuthal angle for each final state for $\theta_\gamma < 5°$

$ep \to e\gamma(p)$: Background subtraction

Let's finally look at the kinematics of the extracted dataset

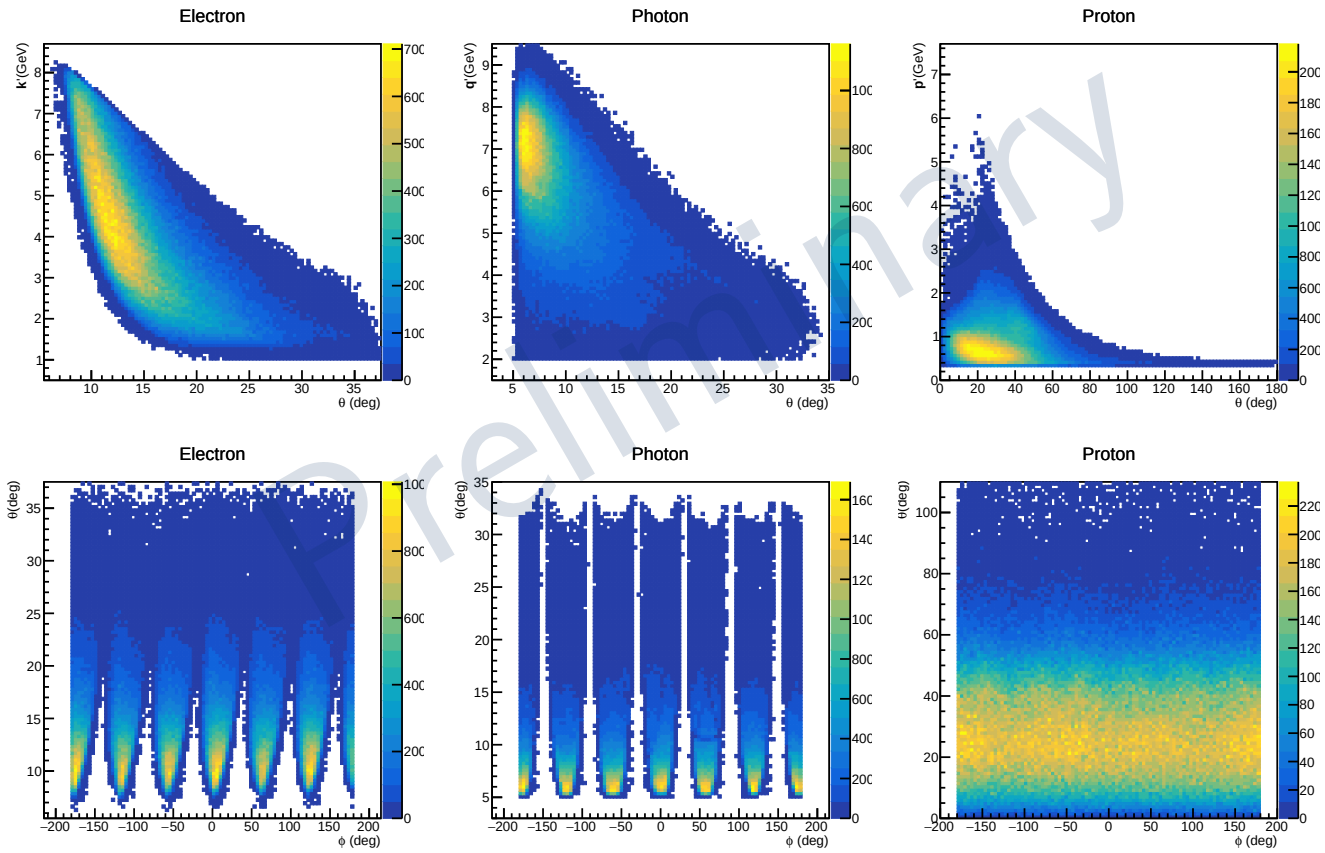

Figure: Momentum of the final particles as a function of the polar angle (first row) and detection polar vs azimuthal angle for each final state for $\theta_\gamma > 5°$

$ep \to e\gamma(p)$: Background subtraction

The training of the BDT results in:

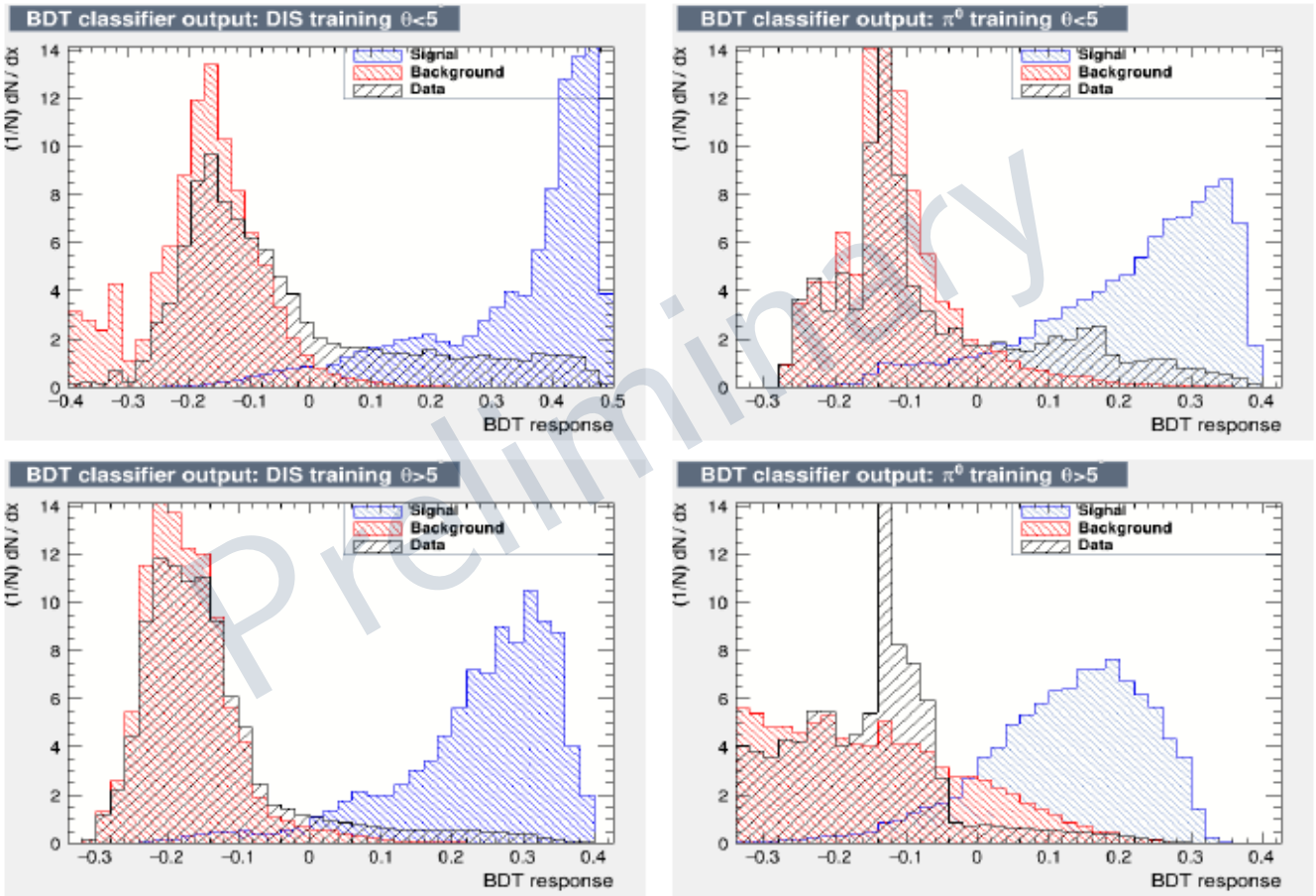

.

Figure: BDT output distributions for the DIS and π^0 background trainings. in the two θ_γ regions.

ROC reconstruction

Using a different sample, we can reconstruct the ROC curve

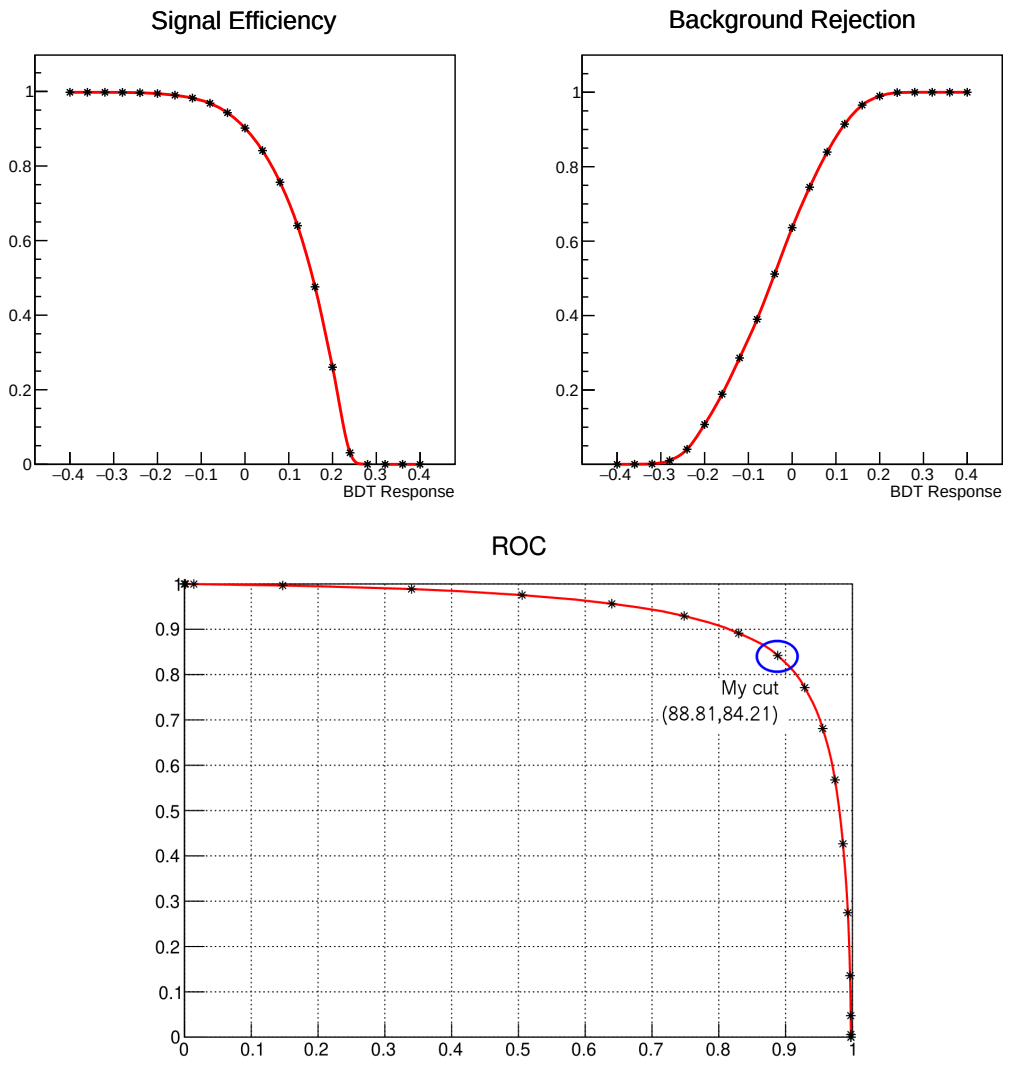

Figure: Reconstructed efficiencies as a function of the BDT response.

ROC reconstruction

From the position on the ROC curve and the number of events, we estimate that the original dataset was 54.58% DVCS and 44.16% π^0 production. So we can create an artificial dataset

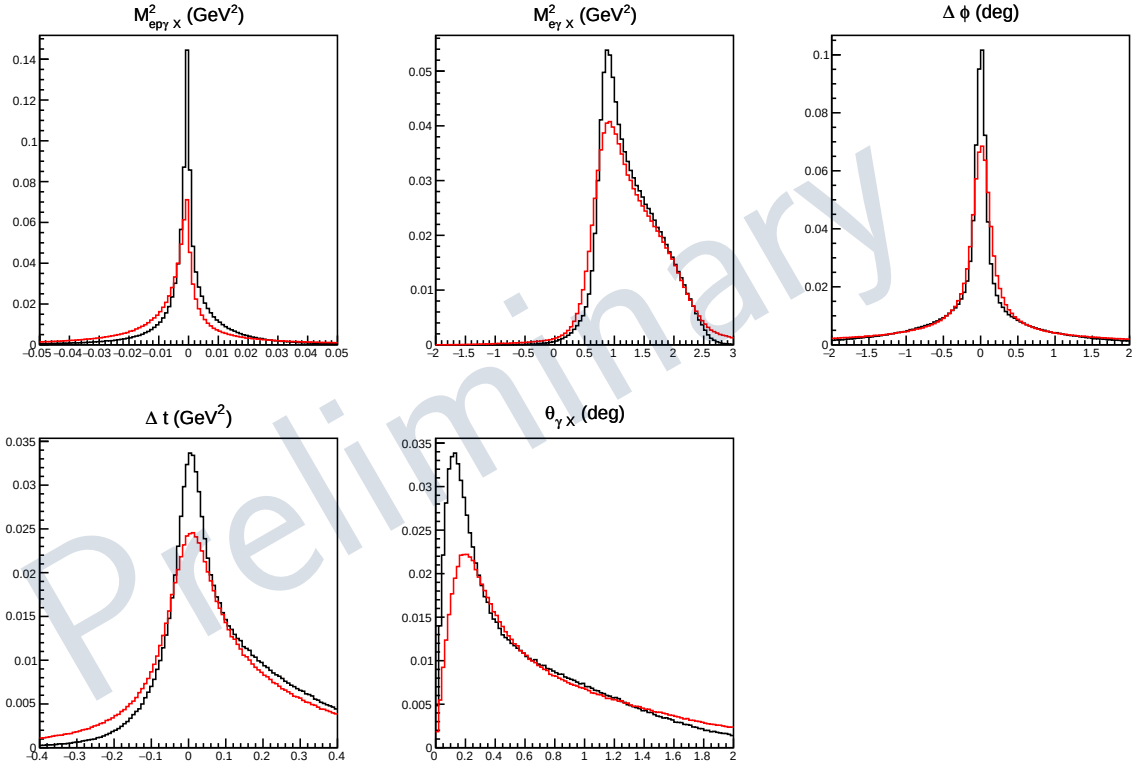

Figure: Normalized DVCS exclusivity variables from data(red) and simulated data (black) before BDT cut.

ROC reconstruction

We observe consistency in the results.

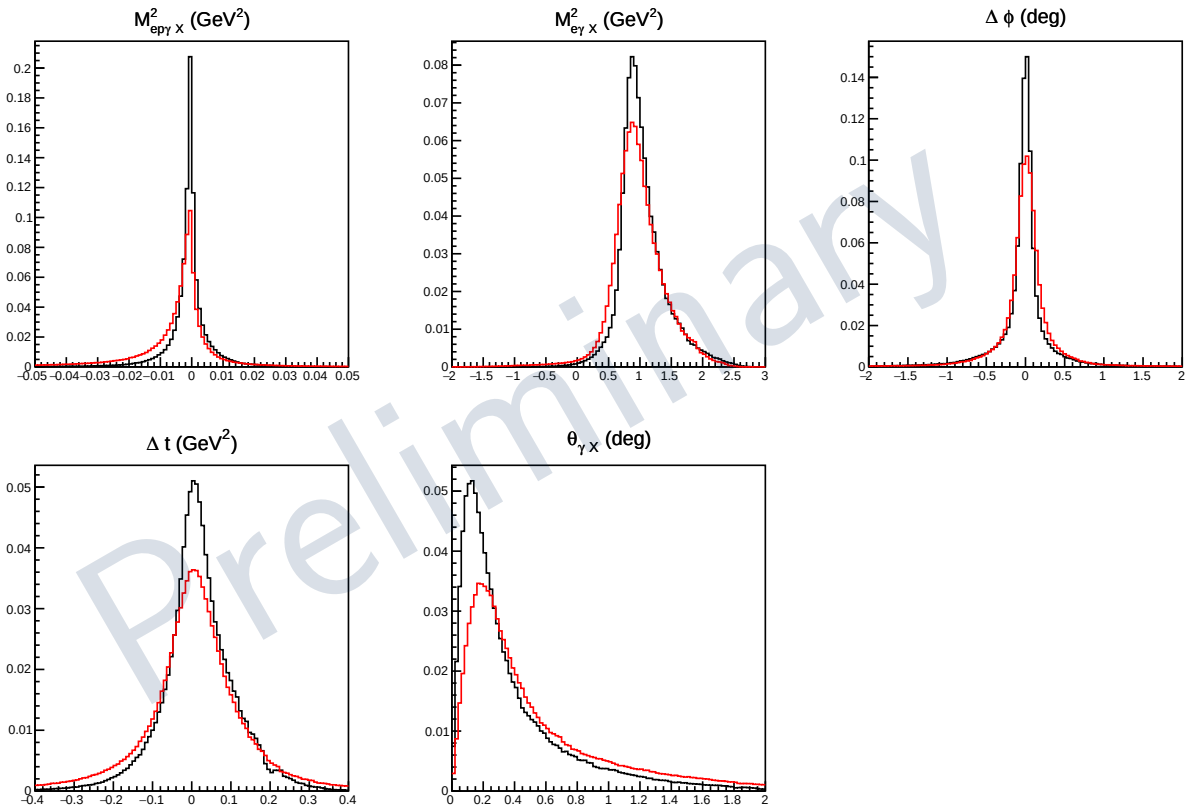

Figure: Normalized DVCS exclusivity variables from data(red) and simulated data (black) after BDT cut.

ROC reconstruction

Looking at each component:

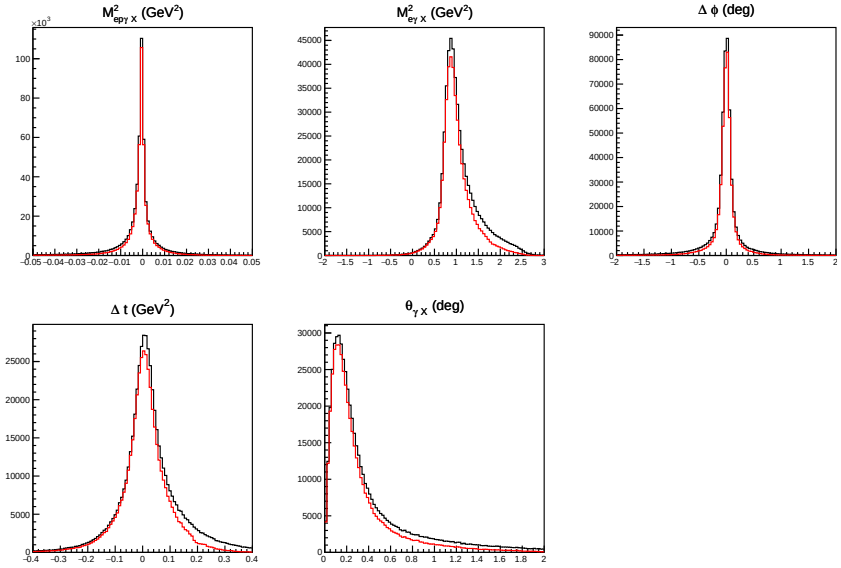

(a) Simulated DVCS before (black) and after (red) BDT cut. signal efficiency: 89.03%, 88.81% expected.

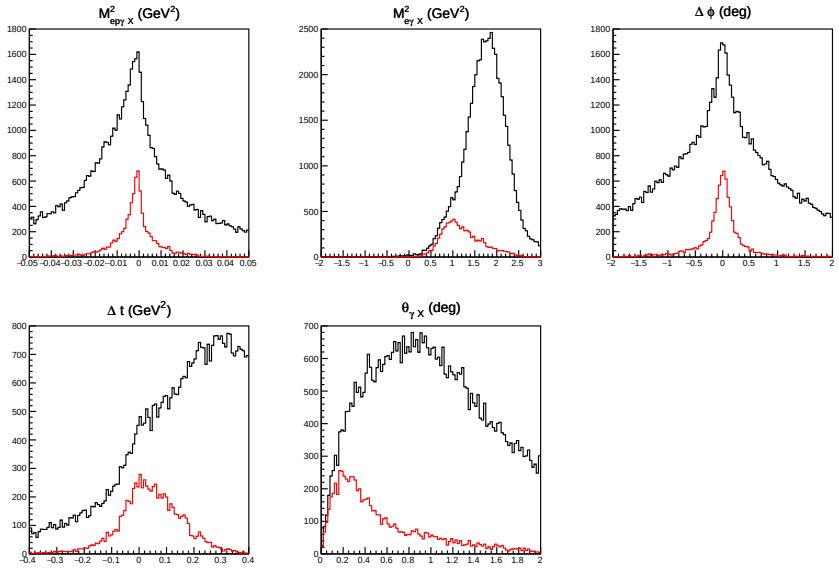

(b) Simulated π^0 data, reconstructed as DVCS, before (black) and after (red) BDT cut.Background rejection: 84.78%, 84.21% expected.

ROC reconstruction

Let us see how π^0 behaves after BDT cut.

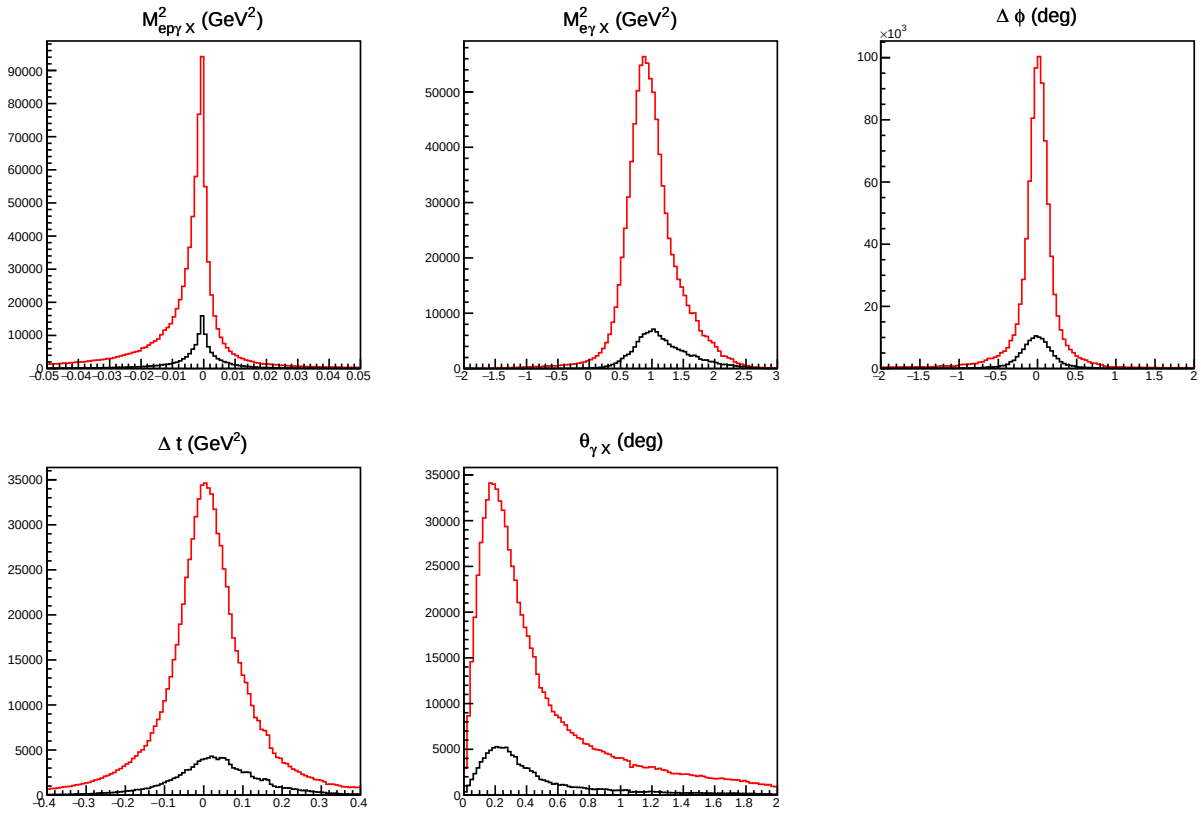

Figure: Data (red) and simulated π^0, reconstructed as DVCS, (black) after BDT cut.

ROC reconstruction

Let us see how π^0 behaves after BDT cut.

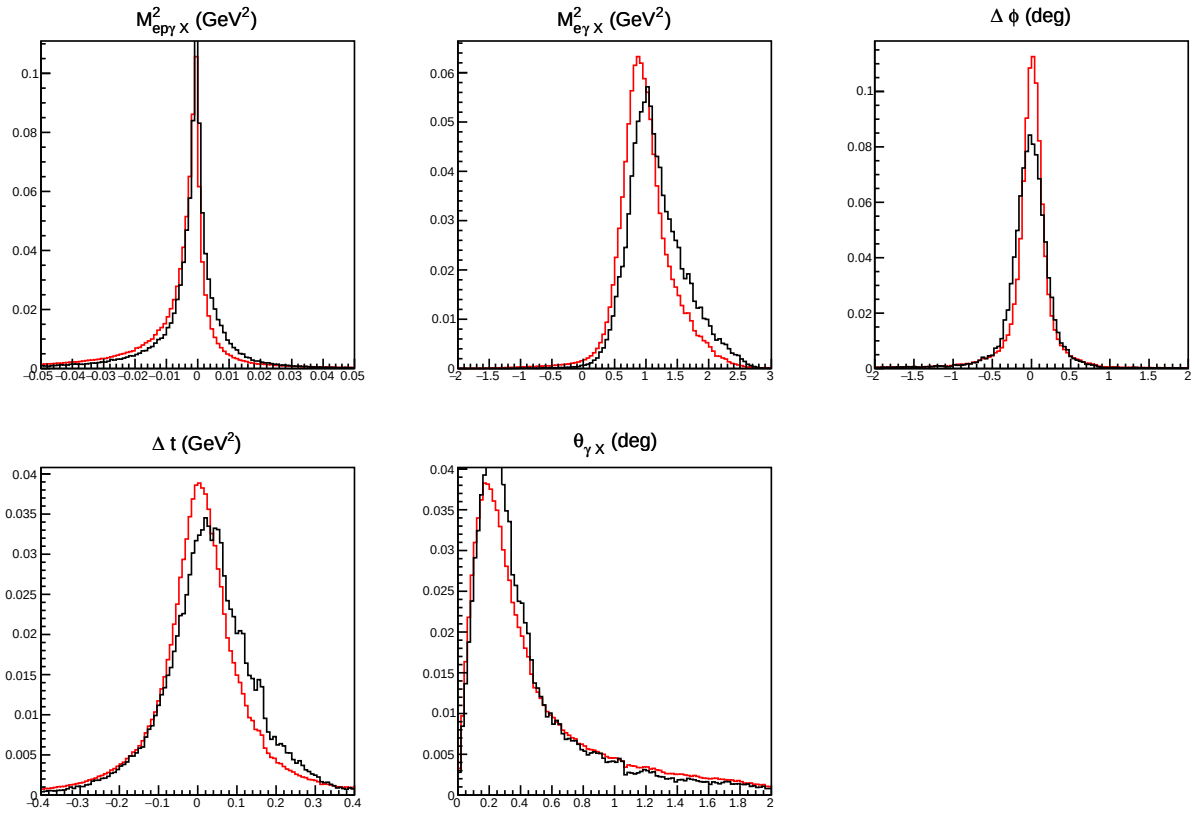

Figure: Normalized Data (red) and simulated π^0, reconstructed as DVCS, (black) after BDT cut.

ROC reconstruction

Moreover, identifying DVCS events is as valuable as identifying π^0 production events:

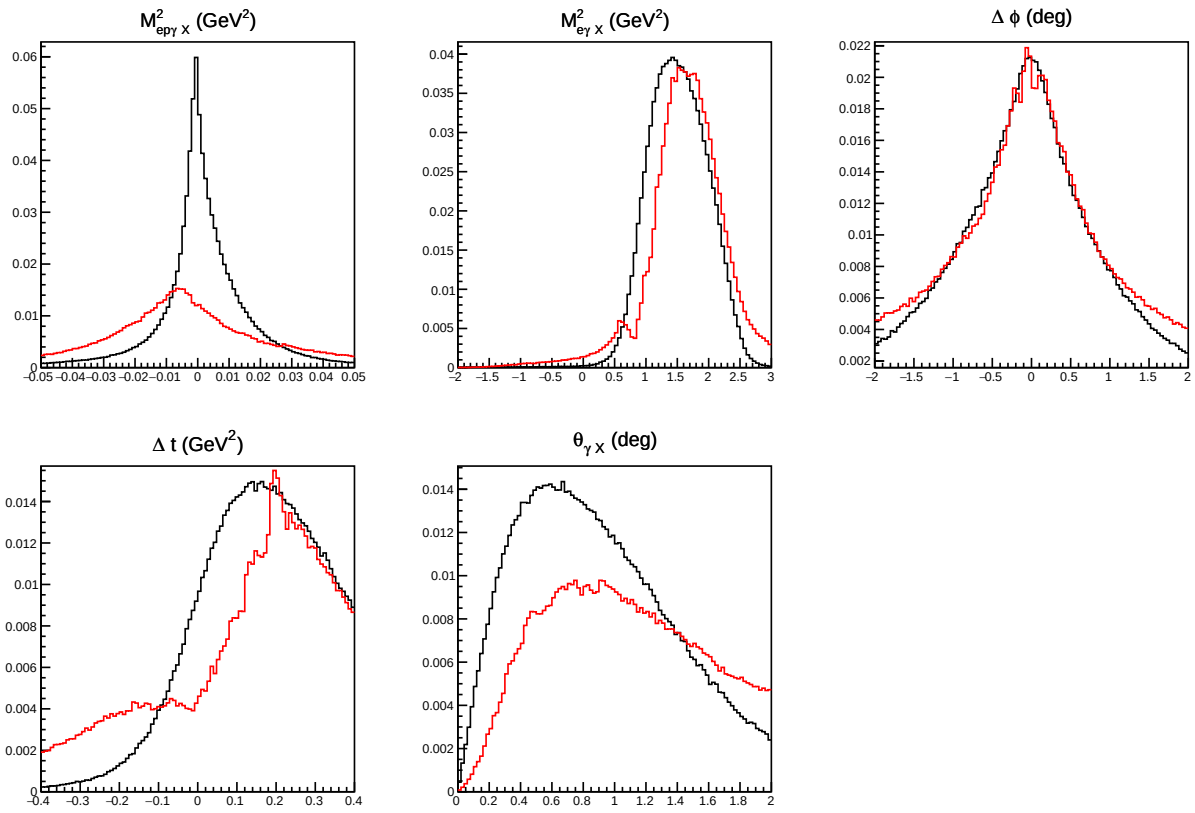

Figure: Simulated π^0 production data, reconstructed as DVCS, (black) and experimental data (red) obtained by inverting the BDT cut.

$ep \to e\gamma(p)$: Data selection

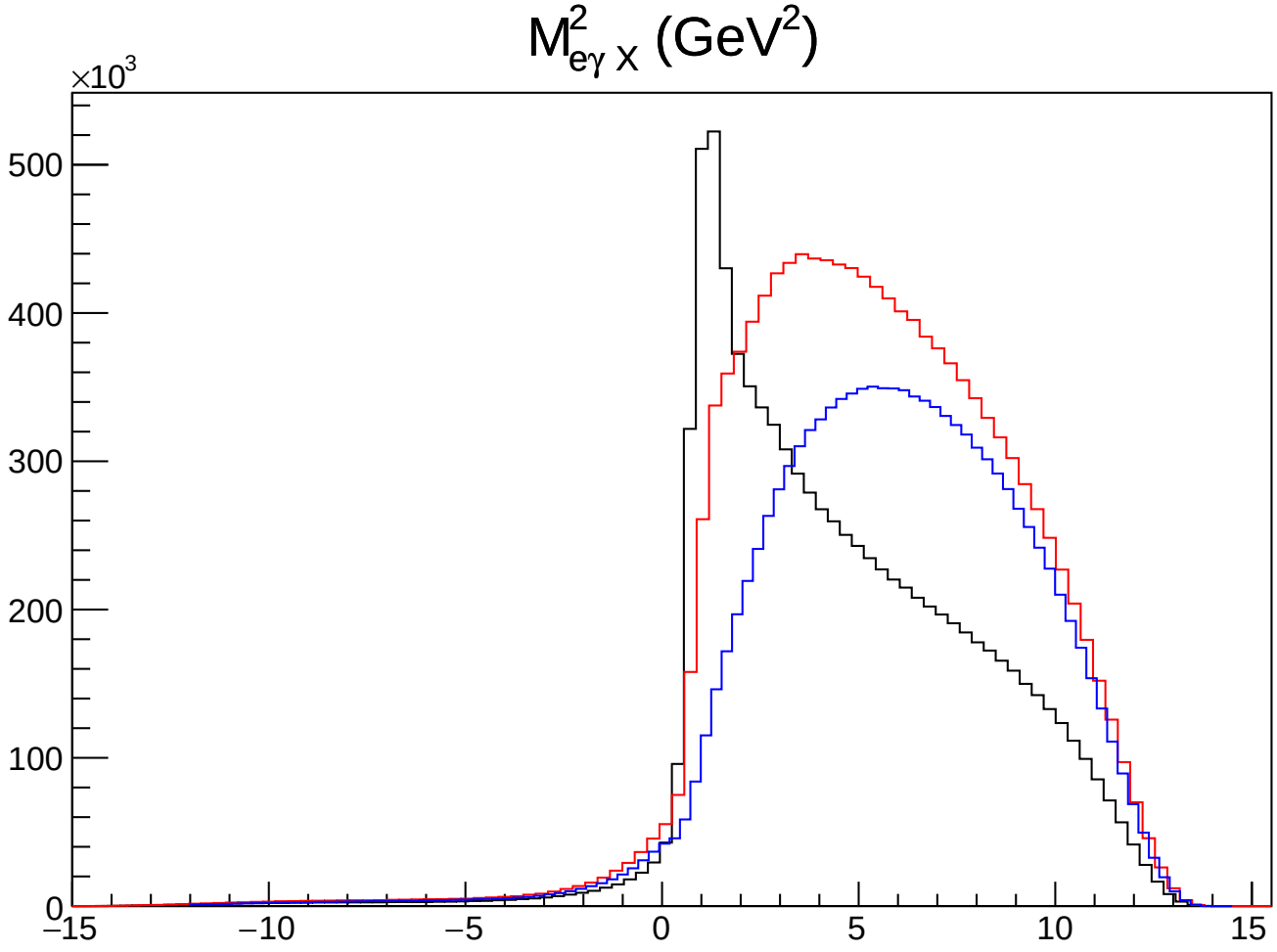

Figure: Missing mass from the process $ep \to e\gamma X$ for events with 1 (black), 2 (red) and 3 (blue) photon detections.

$ep \to e\gamma(p)$: Background subtraction

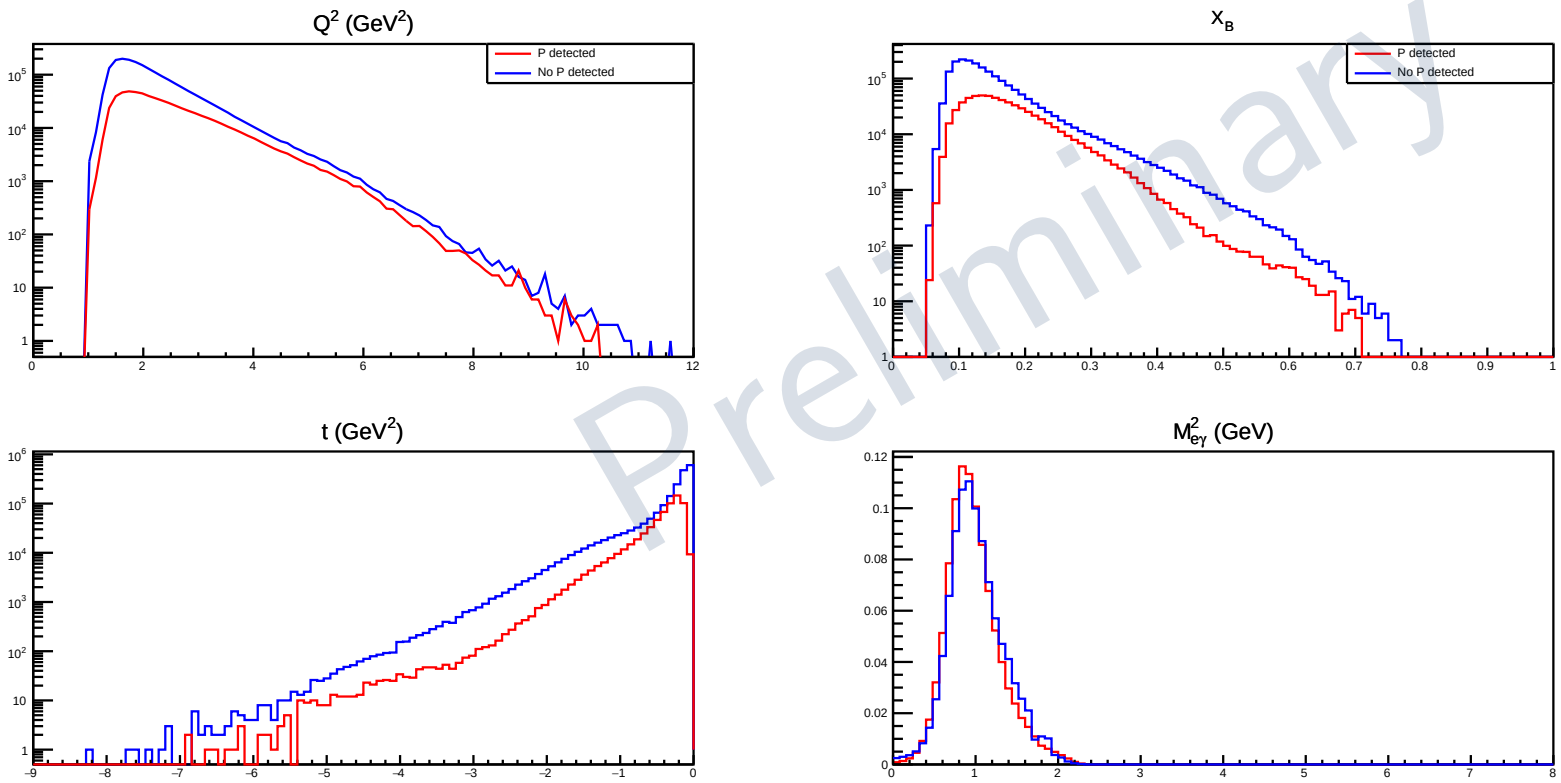

Figure: Q^2, x_B, t and $M^2_{e\gamma}$ distributions, after BDT cut, when the recoil proton is required (red) or not (blue) for $\theta_\gamma < 5°$.

$ep \to e\gamma(p)$: Background subtraction

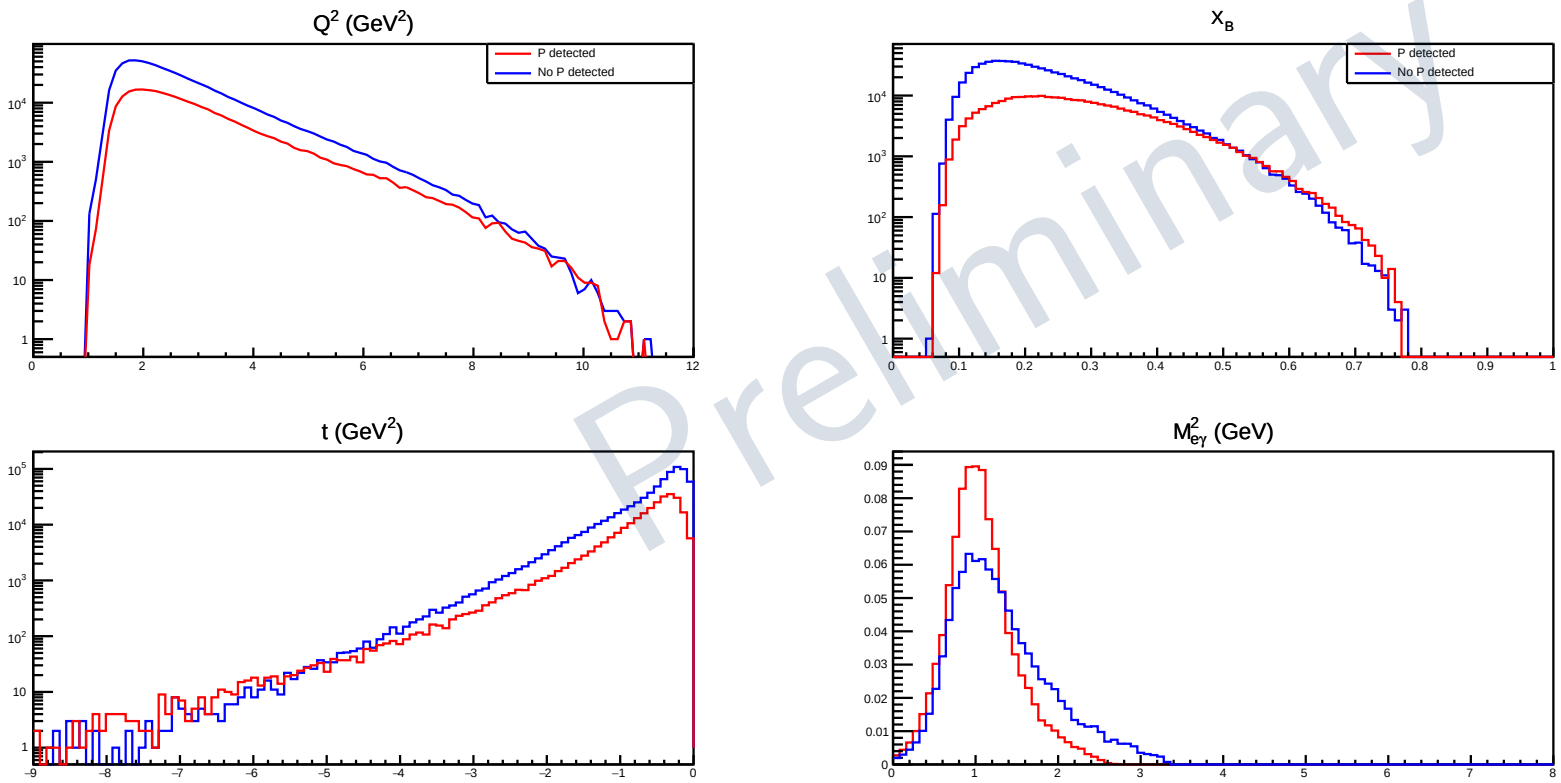

Figure: Q^2, x_B, t and $M^2_{e\gamma}$ distributions, after BDT cut, when the recoil proton is required (red) or not (blue) for $\theta_\gamma > 5°$.

The applied BDT cut leads to the following efficiencies on simulated data:

	$\theta_\gamma < 5°$	Remaining on data	$\theta_\gamma > 5°$	Remaining on data
DVCS	83.5%		86.93%	
π^0	3.64%	<10.3%	16.3%	<100%
DIS	0.044%	<1.2%	0.77%	<9.16%

- DVCS data can be extracted when photons are detected in the Forward Tagger
  - Remaining DIS contamination can be taken into the systematics.
- Remaining contamination is the upper bound coming from the hypothesis that 70% (80%) of the data in the FT (FD) is background data.
- From simulations, we estimate that events at $\theta_\gamma > 5$ contain 3 times more DIS events, 5 times more π^0 events and 3 times **less** DVCS events. (e.g. if 20% of the background is π^0 production, after BDT cut there will be 40% of π^0 contamination.)

Raw Beam Spin Asymmetry

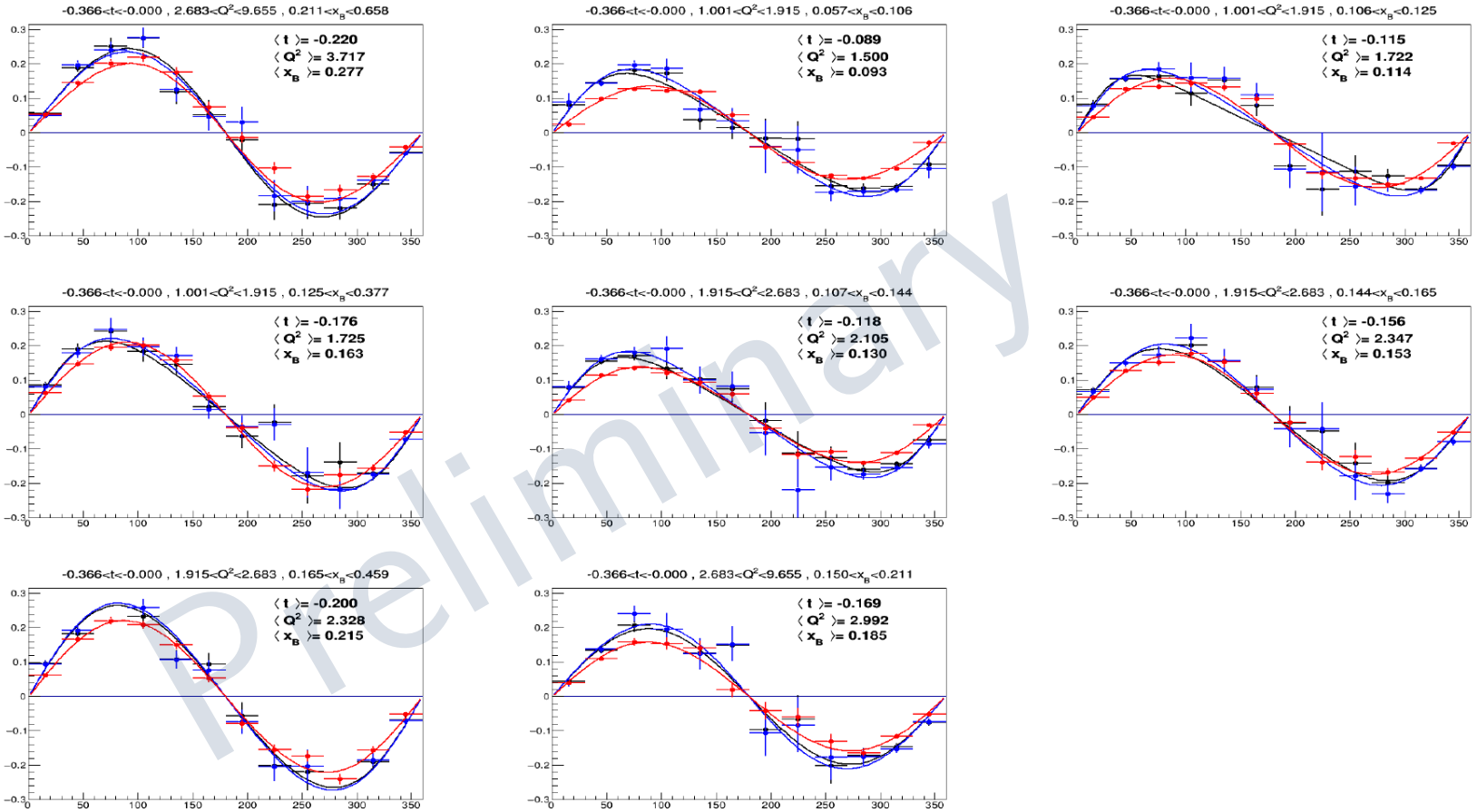

Figure: raw BSA measurements for global training with proton (blue), without proton (red) and **binned training with proton (black)**.